IEEE Access
Multidisciplinary | Rapid Review | Open Access Journal

Received October 7, 2017, accepted January 12, 2018, date of publication January 17, 2018, date of current version February 28, 2018.

Digital Object Identifier 10.1109/ACCESS.2018.2794478

Improved Reconstruction of Low Intensity Magnetic Resonance Spectroscopy With Weighted Low Rank Hankel Matrix Completion

DI GUO[1] AND XIAOBO QU[2]

[1]School of Computer and Information Engineering, Fujian Provincial University Key Laboratory of Internet of Things Application Technology, Xiamen University of Technology, Xiamen 361024, China
[2]Department of Electronic Science, Fujian Provincial Key Laboratory of Plasma and Magnetic Resonance, Xiamen University, Xiamen 361005, China

Corresponding author: Xiaobo Qu (quxiaobo@xmu.edu.cn)

This work was supported in part by the National Natural Science Foundation of China under Grant 61672335, Grant 61601276, Grant 61571380, Grant 61302174, and Grant 6171101498, in part by the Natural Science Foundation of Fujian Province of China under Grant 2016J05205 and Grant 2016J01327, in part by the Important Joint Research Project on Major Diseases of Xiamen City under Grant 3502Z20149032, in part by the Fundamental Research Funds for the Central Universities under Grant 20720150109, in part by Education and Teaching Reform and Construction Project of Xiamen University of Technology under Grant JGZZ201501, and in part by Foundation of Fujian Educational Committee under Grant JAT160358.

ABSTRACT Magnetic resonance spectroscopy (MRS) has many important applications in medical imaging, biology, and chemistry. The 1-D MRS is too crowded for complex samples to retrieve chemical or biological information. The 2-D MRS unfolds the spectrum by introducing another dimension at the cost of much longer data acquisition time. To speed up the data acquisition, one typical way is to sparsely acquire measurements and then reconstruct the spectrum from incomplete observations. Recently, a low rank Hankel matrix (LRHM) approach has shown great potential to reconstruct the spectrum basing on the assumption that the number of spectral peaks is much less than the number of acquired data points. However, low-intensity spectral peaks are compromised in the reconstruction when the data are highly undersampled. In this paper, a weighted LRHM approach is proposed to tackle this problem. A weighted nuclear norm is introduced to better approximate the rank constraint, and a prior signal space is estimated from the prereconstruction to reduce the unknowns in reconstruction. Experimental results on both synthetic and real MRS data demonstrate that the proposed approach can reconstruct low-intensity spectral peaks better than the state-of-the-art LRHM method.

INDEX TERMS Magnetic resonance spectroscopy, sparse sampling, Hankel matrix, low rank, nuclear norm.

I. INTRODUCTION

Magnetic resonance spectroscopy (MRS) provides fruitful information on the physical and chemical properties of atoms or molecules, and it plays important roles in chemistry, biology and medical imaging. The basic form of MRS is in one dimension (1D) which is obtained by performing Fourier transform on the acquired time domain data, also called free induction decay (FID), from the spectrometer [1], [2]. When measuring the structures or chemical environment of molecules on large compounds, e.g. proteins, 1D MRS is always crowded due to the complex coupling or other interactions between atoms or molecules [1], [2]. Thus, multi-dimensional MRS are used to unfold the coupling between different nuclei, e.g. hydrogen, carbon, and oxygen [2]. But, multi-dimensional MRS has one limitation: its data acquisition time is relatively long because it grows rapidly with the increase of resolution and dimensions [3]. To reduce the data acquisition time, one typical way is to sparsely acquire measurements from a spectrometer [4]–[19]. But one has to reconstruct the spectrum from these incomplete observations [4]–[7], [11]–[15], [20]–[23] by exploring prior knowledge on the MRS.

Many reconstruction methods have been proposed for the sparsely sampled MRS. Two emerging state-of-the-art methods are the compressed sensing (CS) [5], [11]–[13] and low rank Hankel matrix (LRHM) methods [15], [16], [20]–[22]. The CS reconstructs the spectrum in frequency domain while the LRHM restores FID in time domain. The CS assumes the spectrum is sparse that contains only a few non-zero valued spectral points, thus narrow peaks are reconstructed

by CS very well. However, broad peaks may be compromised since these signals violate the assumption of sparsity [15]. Alternatively, LRHM supposes the number of spectral peaks is much less than the number of acquired data points and it can faithfully reconstruct both broad and narrow peaks [15]. The LRHM was considered to improve the effective sensitivity in the reconstructed spectra [24] and best theoretically adapted to the exponential property of the FID [25]. LRHM achieves the low rankness by minimizing the nuclear norm of a Hankel matrix converted from the FID [15]. Although this norm is the tightest convex lower bound of the rank, it still deviates from primary goal to minimize the rank of Hankel matrix, i.e. the number of spectral peaks (See Section II. B for more details). Recent development on low rank matrix reconstruction found that a better approximation of the matrix rank can improve the signal reconstruction in practice [26]–[30]. But none of these approaches, as far as we know, has been applied to fast sampling MRS.

In this work, a weighted LRHM approach is introduced to tackle this problem. A prior signal space is first estimated from a pre-reconstruction and then a weighted nuclear norm is introduced to approximate rank constraint on the Hankel matrix. Results on the synthetic and real MRS data show that the low intensity spectral peaks are reconstructed better than the state-of-the-art LRHM does.

Although we mainly work on the spectrum reconstruction, this approach, with proper modifications, may be extended into the low rank Hankel or other structured matrix-based image reconstruction [31]–[35] for sparsely sampled magnetic resonance imaging [36]–[43].

II. BACKGROUND

A. BASICS OF 2D MRS

In the conventional 1D MRS, the spectrometer acquires the FID followed by performing the Fourier transform to obtain the spectrum [2]. The typical data acquisition for a 1D MRS usually takes only several seconds.

To get more information, the 2D MRS are generated as a series of 1D MRS experiments based on two time variables t_1 and t_2 [2], [14], [44] as shown in Fig. 1. For each 1D scan, the sample is excited with pulses first which results in the evolution of magnetization with time t_1 in the indirect dimension (horizontal axis in Fig. 1(b)). Then, the sample is further excited in the mixing period. Finally, the FID signal is recorded as a function of t_2 [2], [14], [44] in the direct dimension (vertical axis in Fig. 1(b)) for a given t1. The overall 2D FID plane is formed by repeating these steps for different time values t_1.

The data acquisition time of 2D MRS is mainly dominated by the total number of data points, N_1, in indirect dimension [45]. To reduce this time, one typical way is to sparsely sample this dimension [15], [22], [45]–[49] by acquiring partial data (Fig. 1(b)). That means, an unduplicated M numbers from $n_j \in \{1, 2, \ldots, N_1\}$ was randomly chosen and the sampling ratio M/N_1 is smaller than 1. To obtain the full spectrum, one has to restore these unsampled data points by introducing prior knowledge on FID or the spectrum.

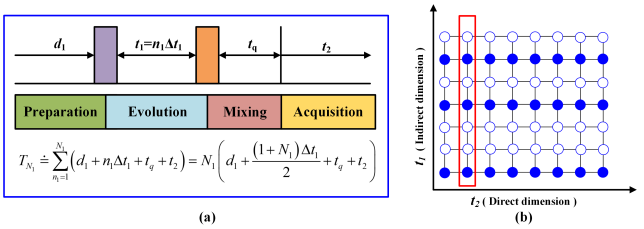

FIGURE 1. The signal excitation scheme and sparse sampling in 2D MRS. (a) The signal excitation scheme, (b) 1D sparse sampling in indirect dimension. Note: The empty (or solid) circle denotes the data point is unsampled (or sampled).

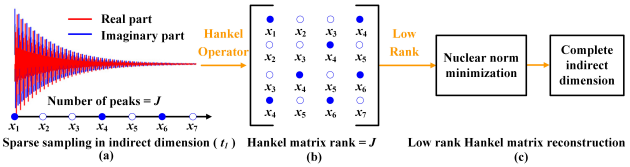

FIGURE 2. Flowchart of the low rank Hankel matrix reconstruction for MRS.

B. MOTIVATION OF THE PROPOSED METHOD

In MRS, the FID signal is usually modeled as the sum of exponential functions as follows [1], [20]–[22], [50], [51]

$$x_n = \sum_{j=1}^{J} a_j e^{i2\pi f_{1,j} n \Delta t_1}, \tag{1}$$

where J is the number of spectral peaks, a_j and $f_{1,j}$ are the complex amplitude and the central frequency of the j^{th} spectral peak, respectively.

The LRHM [15] explores the fundamental property of the FID, i.e., the number of spectral peaks is equal to the number of exponential functions that composing the FID of MRS. By minimizing the rank of the Hankel matrix, LRHM aims at finding a complete FID that corresponds to the minimal number of spectral peaks subject to the acquired data. This method has been extended to reconstruct two-dimensional (2D) or even higher dimensional MRS with considerably fast algorithms [16], [20]–[22].

Figure 2 summarizes the framework of LRHM. A vector, representing each FID in the indrect dimension (the column marked in the red retangle in Fig. 1(b)) is firstly convereted into a Hankel matrix. Then, by exploring the low rank property on this matrix, a complete vector is restored. The whole 2D FID will be recovered by looping the reconstruction along the direct dimension.

In the reconstruction model of the LRHM, the low rank constraint is enforced by minimizing the nuclear norm of the Hankel matrix. Mathematically, each 1D FID $\mathbf{x}$is reconstructed according to [15]

$$\min_{\mathbf{x}} \|\mathbf{R}\mathbf{x}\|_* + \frac{\lambda}{2}\|\mathbf{y}-\mathbf{U}\mathbf{x}\|_2^2, \tag{2}$$

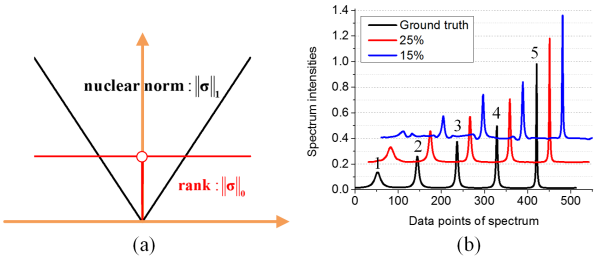

FIGURE 3. Limitations of nuclear norm minimization. (a) Comparisons between rank and nuclear norm of a singular value; (b) Reconstructed MRS using LRHM with nuclear norm minimization. Note: The Arabic numerals denote the identifier on spectral peaks of the ground truth spectrum. From the left to right, the peak widths are from broad to narrow.

where $\mathbf{R}$ denote a Hankel operator converting the FID $\mathbf{x}$ into a Hankel matrix $\mathbf{Rx}$, $\|\cdot\|_*$ represents the nuclear norm (sum of singular values), $\|\cdot\|_2$ represents the l_2 norm, and λ is a regularization parameter that balances the low rankness indicated by the nuclear norm and the data consistency measured with the square of l_2 norm.

However, the LRHM has some limitations both in the mathematical model and MRS applications. First, as a surrogate function of rank, the nuclear norm [26], [27] deviates from the strictly definition of rank (the number of non-zero singular values) as shown in Fig. 3(a). This implies that LRHM does not directly minimizes the number of spectral peaks in MRS subject to the acquired FID. As a result, more sampled data are required in a faithful reconstruction or suboptimal results may be induced when the sampled data are limited [26], [27], [52]. Second, we observed that, when using LRHM, some low intensity spetral peaks may be lost or weakened when data are highly undersampled (Peaks 1 and 2 in Fig. 3(b)).

Fortunately, latest advances in low rank methods have shown that better signal reconstruction may be achieved with a closer approximation of rank [26]–[30] than nuclear norm. Let $\mathbf{X}$ denote a matrix and its singular value decomposition (SVD) be $\mathbf{X} = \mathbf{P\Sigma V}^H$, the nuclear norm of $\mathbf{X}$ is defined as

$$\|\mathbf{X}\|_* = \sum_{l=1}^{L} \sigma_l \tag{3}$$

where the σ_l is the l^{th} non-zero singular values saved in $\mathbf{\Sigma}$.

By introducing a weight $h_l = \sigma_l^{-1}$ on the non-zero singular values, one has

$$\text{rank}\,(\mathbf{X}) = L = \sum_{l=1}^{L} h_l \sigma_l. \tag{4}$$

This implies that one way to approach the rank is to assign a weight that is very close to the inverse proportion of the singular values. Then, a weighted nuclear norm [29], [30], [53] is defined as follows

$$\|\mathbf{X}\|_{\mathbf{w},*} = \sum_{s=1}^{S} w_s \sigma_s, \tag{5}$$

where $\mathbf{w} = [w_1, \cdots, w_s, \cdots, w_S]^T$ includes the weight w_s $(1 \le s \le S)$ for the s^{th} singular values. The notations of the ground truth rank L and singular values σ_l are replaced with S and σ_s respectively, because neither of them are known in practical undersampled signal reconstruction. By minimizing the weighted nuclear norm, signal details have been observed to be reconstructed better than using the nuclear norm [26]–[30].

Motivated by these successful applications of weighted nuclear norm minimization, the focus of this work is to introduce this regularization into the 2D MRS recovery and improve the low intensity signal reconstruction.

III. METHOD

In this section, the FID of MRS is reconstructed using the weighted nuclear norm minimization on the Hankel matrix, which is solved by a fast numerical algorithm.

A. RECONSTRUCTION MODEL

Mathematically, the FID $\mathbf{x}$ is reconstructed from sparsely sampled data by enforcing the low rankness of the corresponding Hankel matrix $\mathbf{Rx}$ as follows

$$\min_{\mathbf{x}} \ \|\mathbf{Rx}\|_{\mathbf{w},*} + \frac{\lambda}{2}\|\mathbf{y} - \mathbf{Ux}\|_2^2, \tag{6}$$

where the regularization parameter λ balances the two terms. This model is named as Weighted Low Rank Hankel Matrix (WLRHM) reconstruction. The core of weighted-LRHM model is to assign proper weights. According to the previous observations [26]–[30], bigger weights should be assigned to those small singular values.

First, the LRHM is used to obtain a pre-reconstruction result $\tilde{\mathbf{x}}$ followed by the SVD according to

$$\mathbf{R}\tilde{\mathbf{x}} = \tilde{\mathbf{P}}\tilde{\mathbf{\Sigma}}\left(\tilde{\mathbf{V}}\right)^H, \tag{7}$$

where the matrix $\tilde{\mathbf{P}}$contains the spectral frequency information of $\tilde{\mathbf{x}}$ [21], [22], [54], [55] and $\tilde{\mathbf{\Sigma}}$ consists the singular values.

Then, a discriminative weight $\mathbf{w} = [w_1, \cdots w_s \cdots, w_S]^T$ is computed as follows

$$w_s = \frac{1}{\tilde{\mathbf{\Sigma}}_s + \varepsilon}, \tag{8}$$

where ε is a small constant that avoids zeros in the denominator and $\tilde{\mathbf{\Sigma}}_s$ is the s^{th} singular values of $\tilde{\mathbf{\Sigma}}$.

B. RECONSTRUCTION ALGORITHM

In the following, how to solve the model will be presented. We adopt the alternating direction minimization method to solve Eq. (6) since it runs fast in Hankel matrix-based MRS reconstruction [15], [20], [22].

Equation (6) is equivalent to the following problem

$$\min_{\mathbf{x},\mathbf{Z}} \|\mathbf{Z}\|_{\mathbf{w},*} + \frac{\lambda}{2}\|\mathbf{y} - \mathbf{Ux}\|_2^2 \quad s.t.\ \mathbf{Rx} = \mathbf{Z} \tag{9}$$

where $\mathbf{Z}$ is a matrix that has the same size of the Hankel matrix $\mathbf{Rx}$.

The augmented Lagrangian form of Eq. (9) becomes

$$G(\mathbf{x}, \mathbf{Z}, \mathbf{D}) = \|\mathbf{Z}\|_{\mathbf{w},*} + \frac{\lambda}{2}\|\mathbf{y} - \mathbf{U}\mathbf{x}\|_2^2 + \langle \mathbf{D}, \mathbf{Rx} - \mathbf{Z}\rangle + \frac{\beta}{2}\|\mathbf{Rx} - \mathbf{Z}\|_F^2. \quad (10)$$

where $\mathbf{D}$ is a dual variable. This minimization turns into alternatingly solve the following sub-problems in an iterative way until the algorithm converges:

$$\begin{cases} \mathbf{x}_{k+1} = \arg\min_{\mathbf{x}} G(\mathbf{x}, \mathbf{Z}_k, \mathbf{D}_k) \\ \mathbf{Z}_{k+1} = \arg\min_{\mathbf{Z}} G(\mathbf{x}_{k+1}, \mathbf{Z}, \mathbf{D}_k), \\ \mathbf{D}_{k+1} = \mathbf{D}_k + (\mathbf{Rx}_{k+1} - \mathbf{Z}_{k+1}). \end{cases} \quad (11)$$

1) Fixing $\mathbf{D}_k$ and $\mathbf{Z}_k$, $\mathbf{x}_{k+1}$is obtained by solving

$$\min_{\mathbf{x}_{k+1}} \frac{\lambda}{2}\|\mathbf{y} - \mathbf{U}\mathbf{x}_{k+1}\|_2^2 + \langle \mathbf{D}_k, \mathbf{Rx} - \mathbf{Z}_k\rangle + \frac{\beta}{2}\|\mathbf{Rx} - \mathbf{Z}_k\|_F^2. \quad (12)$$

whose solution is

$$\mathbf{x}_{k+1} = \left(\lambda\mathbf{U}^T\mathbf{U} + \beta\mathbf{R}^T\mathbf{R}\right)^{-1}\left(\lambda\mathbf{U}^T\mathbf{y} + \beta\mathbf{R}^T\left(\mathbf{Z}_k - \frac{\mathbf{D}_k}{\beta}\right)\right). \quad (13)$$

2) Fixing $\mathbf{D}_k$ and $\mathbf{x}_{k+1}$, $\mathbf{Z}_{k+1}$is obtained by solving

$$\min_{\mathbf{Z}_{k+1}} \|\mathbf{Z}_{k+1}\|_{\mathbf{w},*} + \langle \mathbf{D}_k, \mathbf{Rx}_{k+1} - \mathbf{Z}_{k+1}\rangle + \frac{\beta}{2}\|\mathbf{Rx}_{k+1} - \mathbf{Z}_{k+1}\|_F^2, \quad (14)$$

whose solution is received with a weighted singular thresholding operator [28]–[30], [53] according to

$$\mathbf{Z} = \mathbf{P}\left(\mathbf{\Sigma} - \frac{1}{\beta}\mathrm{diag}(\mathbf{w})\right)_+ \mathbf{V}^H \quad (15)$$

where $\mathbf{P\Sigma V}^H$ is the SVD of $\mathbf{Rx} + \mathbf{D}/\beta$.

3) Fixing $\mathbf{Z}$ and $\mathbf{x}$, update $\mathbf{D}$ according to

$$\mathbf{D} \leftarrow \mathbf{D} + (\mathbf{Rx} - \mathbf{Z}). \quad (16)$$

One can see in Eq. (15) that the low rank reconstruction needs SVD iteratively. We observe that most spectral frequency components of MRS are recovered properly with LRHM. Thus, one may try to project the Hankel matrix onto these pre-estimated frequencies included in $\tilde{\mathbf{P}}$. In our implementation, $\tilde{\mathbf{P}}$ is used to replace the $\mathbf{P}$ in Eq. (15). In another word, $\tilde{\mathbf{P}}$ keep the same in the iterative reconstruction process. This modification potentially reduces the number of unknowns in the low rank reconstruction (A basic low rank reconstruction has to reconstruct three matrices $\mathbf{P}$, $\mathbf{\Sigma}$ and $\mathbf{V}$while our approach only leaves the $\mathbf{\Sigma}$ and $\mathbf{V}$ changed in the iterative process of WLRHM).

To achieve better reconstructions, both the weight $\mathbf{w}$ and matrix $\tilde{\mathbf{P}}$ are suggested to update using WLRHM reconstruction for several times. The overall algorithm of WLRHM are summarized in Table I.

TABLE 1. Reconstruction algorithm of proposed approach.

Initialization: Input $\mathbf{y}$, $\mathbf{R}$, $\mathbf{U}$, set maximal times P of updating weights as 4, convergence condition $\eta_{\text{tol}} = 10^{-6}$, and maximal number of iterations $K = 10^3$. Initialize the solution $\mathbf{x}_0 = \mathbf{U}^T\mathbf{y}$, the dual variable $\mathbf{D}_0 = \mathbf{1}$, the number of iterations $k = 0$ and $\eta_0 = 1$, obtain the pre-reconstruction $\tilde{\mathbf{x}}$ using LRHM.

Main:

For each times $p = 1, 2, \cdots, P$ of updating weights, **do**

1) Estimate $\tilde{\mathbf{P}}$ from $\tilde{\mathbf{x}}$ according to $\mathbf{R}\tilde{\mathbf{x}} = \tilde{\mathbf{P}}\tilde{\mathbf{\Sigma}}\tilde{\mathbf{V}}^H$;

2) Compute $\mathbf{w} = [w_1, \cdots w_s \cdots, w_S]^T$ according to $w_s = \left(\tilde{\mathbf{\Sigma}}_s + \varepsilon\right)^{-1}$;

3) Do weighted nuclear norm reconstruction as follows:
While ($\eta_k \geq \eta_{\text{tol}}$) or ($k < K$), **do**

a) Update $\mathbf{x}_{k+1} = \left(\lambda\mathbf{U}^T\mathbf{U} + \beta\mathbf{R}^T\mathbf{R}\right)^{-1}\left(\lambda\mathbf{U}^T\mathbf{y} + \beta\mathbf{R}^T\left(\mathbf{Z}_k - \mathbf{D}_k/\beta\right)\right)$;

b) Perform $\tilde{\mathbf{P}}\mathbf{\Sigma}_{k+1}\mathbf{V}_{k+1}^H = \mathbf{Rx}_{k+1} + \mathbf{D}_k/\beta$;

c) Update $\mathbf{Z}_{k+1} = \tilde{\mathbf{P}}\left(\mathbf{\Sigma}_{k+1} - \frac{1}{\beta}\mathrm{diag}(\mathbf{w})\right)_+ \mathbf{V}_{k+1}{}^H$;

d) Update $\mathbf{D}_{k+1} = \mathbf{D}_k + (\mathbf{Rx}_{k+1} - \mathbf{Z}_{k+1})$;

e) Compute $\eta_k = \|\mathbf{x}_{k+1} - \mathbf{x}_k\|/\|\mathbf{x}_k\|$ and $k \leftarrow k+1$;

End while

4) Update $\hat{\mathbf{x}} \leftarrow \mathbf{x}_{k+1}$ and $\tilde{\mathbf{x}} \leftarrow \hat{\mathbf{x}}$;

5) Set $k = 0$, $\eta_k = 1$ and $p \leftarrow p+1$;

End for

Output: The reconstructed FID $\hat{\mathbf{x}}$.

The benefits of incorporating weights are analyzed in Fig. 4. Using the proposed approach, spectral correlations are increased for all peaks and the improvement is more obvious for low intensity peaks. More times of updating weights lead to spectral shapes more consistent to the ground truth, however, at the cost of more computation time. In the implementation, the updating times is chosen to be 4 so that reconstructed spectra are restored pretty well without paying too much extra computation time.

IV. RESULTS

The proposed approach will be compared with the state-of-the-art LRHM method [15]. The reconstruction performances will be evaluated on synthetic data and realistic biological MRS measured from proteins.

A. SYNTHETIC DATA

A synthetic FID signal with five spectral peaks (Fig. 5) is generated according to Eq. (1). For all exponential functions, the amplitudes equal to 1, the phases are 0, and the damping factors are 0.01, 0.02, 0.03, 0.04 and 0.08, respectively. Then, the noise with zero mean and standard deviation of 0.005 is

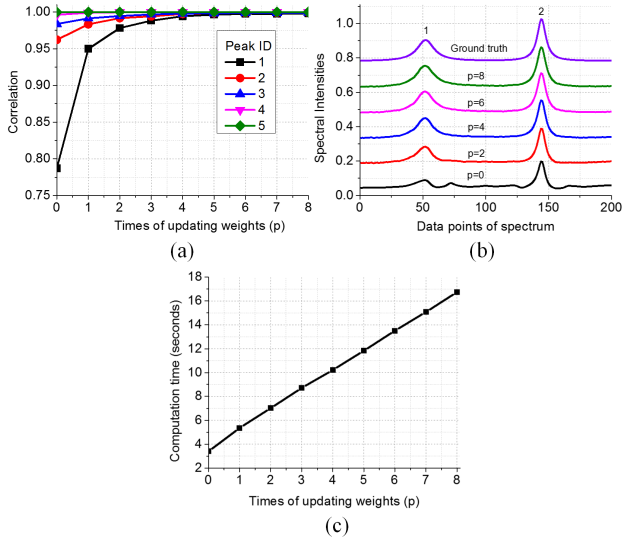

FIGURE 4. Effect of the times of updating weights on (a) peak correlations, (b) spectral shape of low intensity peaks and (c) computation time. Note: Two lowest intensity peaks 1 and 2 in Fig. 3(b) are reconstructed in Fig. 4(b). In the x-axes of (a) and (c), $p = 0$ represents the LRHM reconstruction, $p = 1, \ldots, 8$ means the weighted nuclear norm reconstruction with weights estimated from the $(p-1)^{th}$ reconstruction. Spectra in (b) are equally shifted along vertical axis for better visualization.

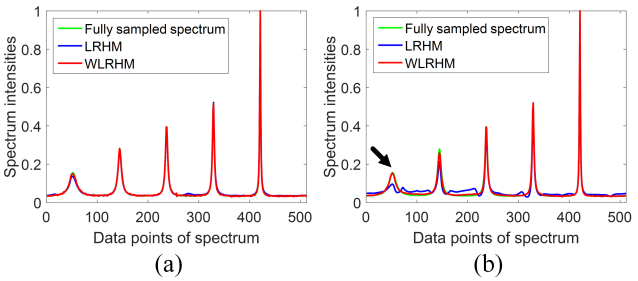

FIGURE 5. Reconstructed spectra when the sampled data is (a) 25% and (b) 15% of the fully sampled data.

added to this spectrum. 15% and 25% of the FID data are randomly sampled according to the Poisson-gap pattern [8].

Fig. 5 shows the reconstructed spectra of the two methods. All the spectral peaks (Fig. 5(a)) are reconstructed very well when the data are sampled sufficiently (25%). But with fewer sampled data (15%), the low intensity peaks (blue line in Fig. 5(b)) are seriously distorted by LRHM, while these peaks (red line in Fig. 5(b)) are recovered much better by WLRHM. The quantitative analysis (Fig. 6) on the spectrum intensities correlation confirms that WLRHM has improved the consistency of all five spectral peaks and this improvement is more obvious for low intensity peaks.

Fig. 7 plots the joint distribution of spectral peak correlations under 100 sampling trials of the two methods. The WLRHM is claimed to yield higher correlation than LRHM if the star point is placed over the dashed line. Otherwise, WLRHM produces lower correlation. The statistical analysis indicates that the new approach outperforms LRHM in most cases.

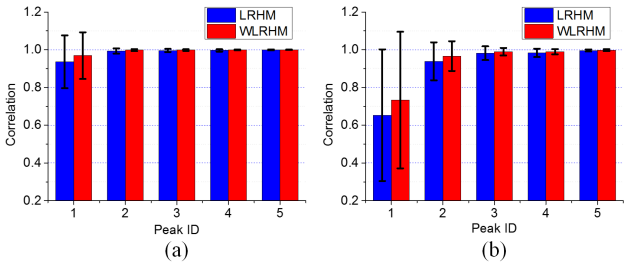

FIGURE 6. Peak intensity correlations for the reconstructed spectra when the sampled data are (a) 25% and (b) 15% of the fully sampled data. Note: The error bars are the standard deviations of correlations over 100 sampling trials.

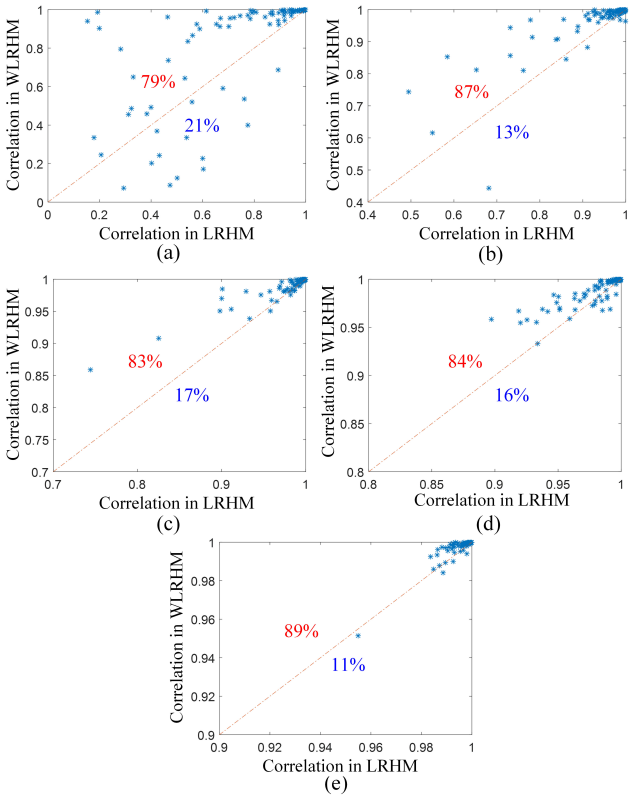

FIGURE 7. The joint distribution of correlation values obtained with LRHM and WLRHM for peaks 1, 2, 3, 4 and 5 in (a), (b), (c), (d) and (e), respectively. Note: 100 sampling trials are conducted when 15% data are sampled. WLRHM is claimed to improve the correlation than LRHM if the star point is placed over the dashed line where the same correlations are reached by both methods. The number marked in red (or blue) is the percentage that the WLRHM reaches higher (or lower) correlation than LRHM.

One may notice that, when the data are highly undersampled, WLRHM may lead to sub-optimal reconstruction of low intensity peaks, e.g. peak 1 in Fig. 7(a), if LRHM reaches correlation that is smaller than 0.8. One explanation is that the weight $\mathbf{w}$ and matrix $\tilde{\mathbf{P}}$ estimated from LRHM is inaccurate in these cases. Therefore, how to improve the robustness of incorporating knowledge from reference signals is a meaningful future work to improve WLRHM.

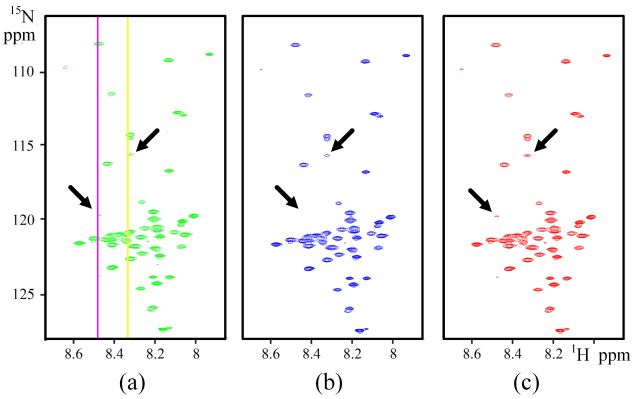

FIGURE 8. Reconstructed 2D HSQC spectrum from 25% data. (a) The fully sampled spectrum; (b) and (c) are reconstructed spectra using the LRHM and WLRHM, respectively.

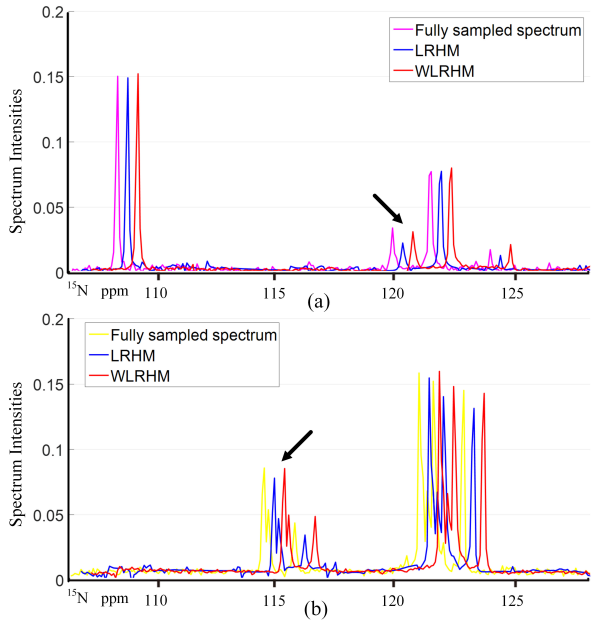

FIGURE 9. 1D traces of reconstructed 2D HSQC spectrum. (a) and (b) are taken at the purple and yellow lines in Fig. 8(a), respectively. Note: 1D traces of reconstruction are shifted for better visualization.

B. MRS DATA

The 2D MRS (Fig. 8(a)) is a ^{1}H-^{15}N HSQC spectrum of the intrinsically disordered cytosolic domain of human CD79b protein from the B-cell receptor. This 2D spectrum is measured at the following conditions: 300 μM ^{15}N-^{13}C labeled sample of cytosolic CD79b in 20 mM sodium phosphate buffer, pH 6.7 was used to obtain the fully sampled 2D ^{1}H-^{15}N HSQC with 256 complex points in the ^{15}N dimension at 55 °C on 800 MHz Bruker AVANCE III HD spectrometer equipped with 3 mm CPTCI cryoprobe [56]. The size of the 2D FID is 256 in indirect dimension and 110 in direct dimension. Only 25% of data are randomly sampled in the indirect dimension according to the Poisson-gap pattern [8].

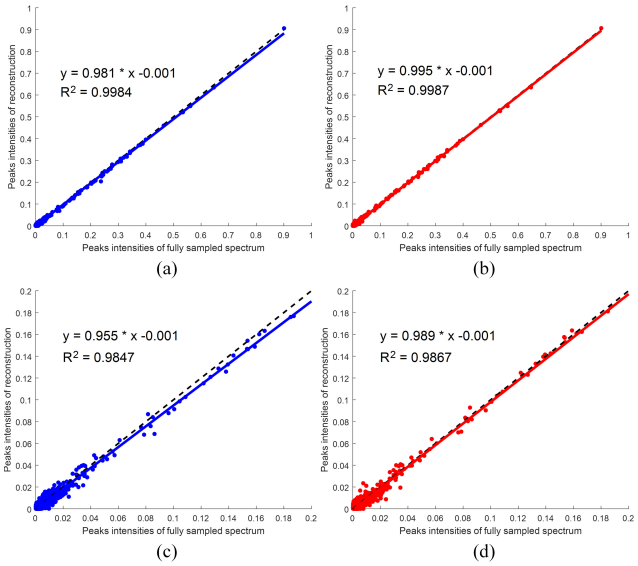

FIGURE 10. Peak intensities correlation between fully sampled spectrum and reconstructed spectrum on the 2D HSQC. (a) and (b) are estimated with all peaks using LRHM and WLRHM, respectively; (c) and (d) are estimated with partial peaks of low intensities at a range of [0, 0.2] using LRHM and WLRHM, respectively. Note: The notation R^2 denotes the Pearsons linear correlation coefficient of fitted curve. The closer that the value of R^2 approaches to 1, the stronger the correlation between the fully sampled spectra and reconstructed spectra is.

The reconstructed 2D MRS is shown in Fig. 8. The WLRHM reconstructs the spectral peaks (Fig. 8(c)) better than the LRHM (Fig. 8(b)), particularly for the marked spectral peaks. Representative 1D traces (Fig. 9(d)) clearly depict that low intensity peaks are compromised by LRHM but faithfully recovered by the proposed approach. The quantitative analysis on the spectrum intensities correlation in Fig. 10 also confirms that WLRHM improve low intensity spectrum (Fig. 10(c) and (d)) although the improvement for all peaks (Fig. 10(a) and (b)) is not significant. These observations imply that the proposed method can reconstruct more consistent spectrum to the fully sampled 2D MRS.

V. CONCLUSION

A weighted low rank Hankel matrix completion method is introduced to reconstruct the sparsely sampled data in fast magnetic resonance spectroscopy. The weights are learnt from pre-reconstruction using LRHM. The low rank model is then solved with a fast numerical algorithm. Besides, frequency components are kept during the SVD in an iterative process of the algorithm. Experimental results show the great potential of the proposed approach in the reconstruction of the low intensity spectral peaks. Thus, this method provides a solution to improve the potential sensitivity in magnetic resonance spectroscopy.

ACKNOWLEDGEMENTS

The authors are grateful to Prof. Vladislav Yu. Orekhov for sharing the 2D HSQC data [15], [56] and appreciate the reviewers' valuable suggestions.

REFERENCES

[1] J. C. Hoch and A. S. Stern, *NMR Data Processing*. Hoboken, NJ, USA: Wiley, 1996.

[2] J. Keeler, *Understanding NMR Spectroscopy*. New York, NY, USA: Wiley, 2005.

[3] V. Y. Orekhov and V. A. Jaravine, "Analysis of non-uniformly sampled spectra with multi-dimensional decomposition," *Prog. Nucl. Magn. Reson. Spectrosc.*, vol. 59, no. 3, pp. 271–292, 2011.

[4] J. W. Yoon and S. J. Godsill, "Bayesian inference for multidimensional NMR image reconstruction," presented at the Eur. Signal Process. Conf. (EUSIPCO), Florence, Italy, Sep. 2006.

[5] I. Drori, "Fast ℓ_1 minimization by iterative thresholding for multidimensional NMR spectroscopy," *Eurasip J. Adv. Signal Process.*, vol. 2007, Dec. 2007, Art. no. 020248.

[6] M. Mobli and J. C. Hoch, "Maximum entropy spectral reconstruction of nonuniformly sampled data," *Concepts Magn. Reson. A*, vol. 32A, no. 6, pp. 436–448, Nov. 2008.

[7] Y. Matsuki, M. T. Eddy, and J. Herzfeld, "Spectroscopy by integration of frequency and time domain information for fast acquisition of high-resolution dark spectra," *J. Amer. Chem. Soc.*, vol. 131, no. 13, pp. 4648–4656, Apr. 2009.

[8] S. G. Hyberts, K. Takeuchi, and G. Wagner, "Poisson-gap sampling and forward maximum entropy reconstruction for enhancing the resolution and sensitivity of protein NMR data," *J. Amer. Chem. Soc.*, vol. 132, no. 7, pp. 2145–2147, 2010.

[9] B. Jiang *et al.*, "Gridding and fast Fourier transformation on non-uniformly sparse sampled multidimensional NMR data," *J. Magn. Reson.*, vol. 204, no. 1, pp. 165–168, May 2010.

[10] K. Kazimierczuk, J. Stanek, A. Zawadzka-Kazimierczuk, and W. Koźmiński, "Random sampling in multidimensional NMR spectroscopy," *Prog. Nucl. Magn. Reson. Spectrosc.*, vol. 57, no. 4, pp. 420–434, 2010.

[11] D. J. Holland, M. J. Bostock, L. F. Gladden, and D. Nietlispach, "Fast multidimensional NMR spectroscopy using compressed sensing," *Angew. Chem. Int. Ed.*, vol. 50, no. 29, pp. 6548–6551, Jul. 2011.

[12] K. Kazimierczuk and V. Y. Orekhov, "Accelerated NMR spectroscopy by using compressed sensing," *Angew. Chem. Int. Ed.*, vol. 50, no. 24, pp. 5556–5559, Jun. 2011.

[13] X. Qu, X. Cao, D. Guo, and Z. Chen, "Compressed sensing for sparse magnetic resonance spectroscopy," presented at the 18th Sci. Meeting Int. Soc. Magn. Reson. Med. (ISMRM), Stockholm, Sweden, 2010, p. 3371.

[14] X. Qu, D. Guo, X. Cao, S. Cai, and Z. Chen, "Reconstruction of self-sparse 2D NMR spectra from undersampled data in the indirect dimension," *Sensors*, vol. 11, no. 9, pp. 8888–8909, 2011.

[15] X. Qu, M. Mayzel, J.-F. Cai, Z. Chen, and V. Orekhov, "Accelerated NMR spectroscopy with low-rank reconstruction," *Angew. Chem. Int. Ed.*, vol. 54, no. 3, pp. 852–854, Jan. 2015.

[16] D. Guo, H. Lu, and X. Qu, "A fast low rank Hankel matrix factorization reconstruction method for non-uniformly sampled magnetic resonance spectroscopy," *IEEE Access*, vol. 5, pp. 16033–16039, 2017.

[17] M. Mayzel, J. Rosenlöw, L. Isaksson, and V. Y. Orekhov, "Time-resolved multidimensional NMR with non-uniform sampling," *J. Biomol. NMR*, vol. 58, no. 2, pp. 129–139, Feb. 2014.

[18] R. Brüschweiler and F. Zhang, "Covariance nuclear magnetic resonance spectroscopy," *J. Chem. Phys.*, vol. 120, no. 11, pp. 5253–5260, 2004.

[19] M. Mayzel, K. Kazimierczuk, and V. Y. Orekhov, "The causality principle in the reconstruction of sparse NMR spectra," *Chem. Commun.*, vol. 50, no. 64, pp. 8947–8950, 2014.

[20] H. Lu *et al.*, "Low rank enhanced matrix recovery of hybrid time and frequency data in fast magnetic resonance spectroscopy," *IEEE Trans. Biomed. Eng.*, to be published, doi: 10.1109/TBME.2017.2719709.

[21] X. Qu, J. Ying, J.-F. Cai, and Z. Chen, "Accelerated magnetic resonance spectroscopy with Vandermonde factorization," presented at the 39th Annu. Int. Conf. IEEE Eng. Med. Biol. Soc. (EMBC), Jeju Province, Korea, Jul. 2017, pp. 3537–3540.

[22] J. Ying *et al.*, "Hankel matrix nuclear norm regularized tensor completion for N-dimensional exponential signals," *IEEE Trans. Signal Process.*, vol. 65, no. 14, pp. 3702–3717, Jul. 2017.

[23] Y. Li *et al.*, "Covariance spectroscopy with a non-uniform and consecutive acquisition scheme for signal enhancement of the NMR experiments," *J. Magn. Reson.*, vol. 217, pp. 106–111, Apr. 2012.

[24] T. E. Linnet and K. Teilum, "Non-uniform sampling of NMR relaxation data," *J. Biomolecular NMR*, vol. 64, no. 2, pp. 165–173, Feb. 2016.

[25] A. Shchukina, P. Kasprzak, R. Dass, M. Nowakowski, and K. Kazimierczuk, "Pitfalls in compressed sensing reconstruction and how to avoid them," *J. Biomolecular NMR*, vol. 68, no. 2, pp. 79–98, 2017.

[26] B. Recht, M. Fazel, and P. A. Parrilo, "Guaranteed minimum-rank solutions of linear matrix equations via nuclear norm minimization," *SIAM Rev.*, vol. 52, no. 3, pp. 471–501, 2010.

[27] M. Fazel, T. Pong, D. Sun, and P. Tseng, "Hankel matrix rank minimization with applications to system identification and realization," *SIAM J. Matrix Anal. Appl.*, vol. 34, no. 3, pp. 946–977, 2013.

[28] W. Dong, G. Shi, X. Li, Y. Ma, and F. Huang, "Compressive sensing via nonlocal low-rank regularization," *IEEE Trans. Image. Process.*, vol. 32, no. 8, pp. 3618–3632, Aug. 2014.

[29] S. Gu, Q. Xie, D. Meng, W. Zuo, X. Feng, and L. Zhang, "Weighted nuclear norm minimization and its applications to low level vision," *Int. J. Comput. Vis.*, vol. 121, no. 2, pp. 183–208, Jan. 2017.

[30] Z. Zha *et al.*, "Analyzing the group sparsity based on the rank minimization methods," presented at the IEEE Int. Conf. Multimedia Expo (ICME), Jul. 2017, pp. 883–888.

[31] J. P. Haldar, "Low-rank modeling of local k-space neighborhoods (LORAKS) for constrained MRI," *IEEE Trans. Med. Imag.*, vol. 33, no. 3, pp. 668–681, Mar. 2014.

[32] P. J. Shin *et al.*, "Calibrationless parallel imaging reconstruction based on structured low-rank matrix completion," *Magn. Reson. Med.*, vol. 72, no. 4, pp. 959–970, Oct. 2014.

[33] G. Ongie and M. Jacob, "Off-the-grid recovery of piecewise constant images from few Fourier samples," *SIAM J. Imag. Sci.*, vol. 9, no. 3, pp. 1004–1041, 2016.

[34] Z.-P. Liang, E. M. Haacke, and C. W. Thomas, "High-resolution inversion of finite Fourier transform data through a localised polynomial approximation," *Inverse Problems*, vol. 5, no. 5, p. 831, 1989.

[35] K. H. Jin, D. Lee, and J. C. Ye, "A general framework for compressed sensing and parallel MRI using annihilating filter based low-rank Hankel matrix," *IEEE Trans. Comput. Imag.*, vol. 2, no. 4, pp. 480–495, Dec. 2016.

[36] Z.-P. Liang, "Spatiotemporal imaging with partially separable functions," in *Proc. 4th IEEE Int. Symp. Biomed. Imag., Nano Macro (ISBI)*, Arlington, VA, USA, Apr. 2007, pp. 988–991.

[37] M. Lustig, D. Donoho, and J. M. Pauly, "Sparse MRI: The application of compressed sensing for rapid MR imaging," *Magn. Reson. Med.*, vol. 58, no. 6, pp. 1182–1195, 2007.

[38] D. Liang, B. Liu, J. Wang, and L. Ying, "Accelerating SENSE using compressed sensing," *Magn. Reson. Med.*, vol. 62, no. 6, pp. 1574–1584, Dec. 2009.

[39] X. Qu *et al.*, "Undersampled MRI reconstruction with patch-based directional wavelets," *Magn. Reson. Imag.*, vol. 30, no. 7, pp. 964–977, Sep. 2012.

[40] X. Qu, Y. Hou, F. Lam, D. Guo, J. Zhong, and Z. Chen, "Magnetic resonance image reconstruction from undersampled measurements using a patch-based nonlocal operator," *Med. Image Anal.*, vol. 18, no. 6, pp. 843–856, Aug. 2014.

[41] Y. Liu, Z. Zhan, J.-F. Cai, D. Guo, Z. Chen, and X. Qu, "Projected iterative soft-thresholding algorithm for tight frames in compressed sensing magnetic resonance imaging," *IEEE Trans. Med. Imag.*, vol. 35, no. 9, pp. 2130–2140, Sep. 2016.

[42] Z. Zhan, J.-F. Cai, D. Guo, Y. Liu, Z. Chen, and X. Qu, "Fast multiclass dictionaries learning with geometrical directions in MRI reconstruction," *IEEE Trans. Biomed. Eng.*, vol. 63, no. 9, pp. 1850–1861, Sep. 2016.

[43] Y. Zhang, Z. Dong, P. Phillips, S. Wang, G. Ji, and J. Yang, "Exponential wavelet iterative shrinkage thresholding algorithm for compressed sensing magnetic resonance imaging," *Inf. Sci.*, vol. 322, pp. 115–132, Nov. 2015.

[44] W. P. Aue, E. Bartholdi, and R. R. Ernst, "Two-dimensional spectroscopy. Application to nuclear magnetic resonance," *J. Chem. Phys.*, vol. 64, no. 5, pp. 2229–2246, 1976.

[45] M. Mobli and J. C. Hoch, "Nonuniform sampling and non-Fourier signal processing methods in multidimensional NMR," *Prog. Nucl. Magn. Reson. Spectrosc.*, vol. 83, pp. 21–41, Nov. 2014.

[46] J. C. Hoch, M. W. Maciejewski, M. Mobli, A. D. Schuyler, and A. S. Stern, "Nonuniform sampling and maximum entropy reconstruction in multidimensional NMR," *Accounts Chem. Res.*, vol. 47, no. 2, pp. 708–717, 2014.
[47] Q. Wu, B. E. Coggins, and P. Zhou, "Unbiased measurements of reconstruction fidelity of sparsely sampled magnetic resonance spectra," *Nature Commun.*, vol. 7, Jul. 2016, Art. no. 12281.
[48] B. E. Coggins, J. W. Werner-Allen, A. Yan, and P. Zhou, "Rapid protein global fold determination using ultrasparse sampling, high-dynamic range artifact suppression, and time-shared NOESY," *J. Amer. Chem. Soc.*, vol. 134, no. 45, pp. 18619–18630, 2012.
[49] J. Ying, F. Delaglio, D. A. Torchia, and A. Bax, "Sparse multidimensional iterative lineshape-enhanced (SMILE) reconstruction of both nonuniformly sampled and conventional NMR data," *J. Biomol. NMR*, vol. 68, no. 2, pp. 101–118, Jun. 2017.
[50] P. Koehl, "Linear prediction spectral analysis of NMR data," in *Prog. Nucl. Magn. Reson. Spectrosc.*, vol. 34. 1999, pp. 257–299.
[51] H. M. Nguyen, X. Peng, M. N. Do, and Z.-P. Liang, "Denoising MR spectroscopic imaging data with low-rank approximations," *IEEE Trans. Biomed. Eng.*, vol. 60, no. 1, pp. 78–89, Jan. 2013.
[52] J.-F. Cai, T. Wang, and K. Wei, "Fast and provable algorithms for spectrally sparse signal reconstruction via low-rank Hankel matrix completion," *Appl. Comput. Harmon. Anal.*, to be published, doi: 10.1016/j.acha.2017.04.004.
[53] S. Gu, L. Zhang, W. Zuo, and X. Feng, "Weighted nuclear norm minimization with application to image denoising," in *Proc. IEEE Conf. Comput. Vis. Pattern Recognit. (CVRP)*, vol. 14. Jun. 2014, pp. 2862–2869.
[54] J.-F. Cai, X. Qu, W. Xu, and G.-B. Ye, "Robust recovery of complex exponential signals from random Gaussian projections via low rank Hankel matrix reconstruction," *Appl. Comput. Harmon. Aanl.*, vol. 41, no. 2, pp. 470–490, Sep. 2016.
[55] W. W. F. Pijnappel, A. van den Boogaart, R. de Beer, and D. van Ormondt, "SVD-based quantification of magnetic resonance signals," *J. Magn. Reson.*, vol. 97, no. 1, pp. 122–134, Mar. 1992.
[56] L. Isaksson *et al.*, "Highly efficient NMR assignment of intrinsically disordered proteins: Application to B- and T cell receptor domains," *PLoS ONE*, vol. 8, no. 5, p. e62947, 2013.

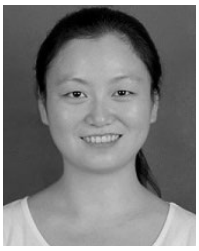

DI GUO received the B.S. and Ph.D. degrees in communication engineering from Xiamen University, China, in 2005 and 2012, respectively. From 2009 to 2011, she was a Visiting Scientist with the Department of Electrical Engineering, University of Washington, Seattle, WA, USA. She is currently an Associate Professor with the Department of Computer Science and Technology, Xiamen University of Technology, China. Her research interests include signal and image processing and their applications in biomedical engineering, wireless sensor networks, and Internet of Things. She received the IBM Distinguished Student Award in 2012.

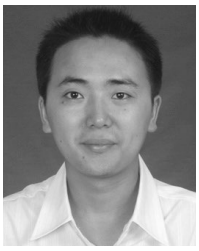

XIAOBO QU received the B.S. degree and the Ph.D. degree in communication engineering from Xiamen University, China, in 2006 and 2011, respectively. From 2009 to 2011, he was a Visiting Scholar with the Department of Electrical and Computer Engineering, University of Illinois at Urbana–Champaign. In 2014, he joined the Swedish NMR Centre, University of Gothenburg, Sweden, as a Visiting Scientist. Since 2012, he has been a Faculty Member with Xiamen University, where he is currently an Associate Professor with the Research Center of Magnetic Resonance and Medical Imaging and the Research Center for Molecular Imaging and Translational Medicine, Department of Electronic Science. His research interests include magnetic resonance imaging and spectroscopy, signal and image representations, wavelets, inverse problems, and computational imaging. He is a member of the ISMRM, the IEEE EMBS, and the SPS. He is also the Section Editor of the *BMC Medical Imaging* and on the Editorial Board of *Quantitative Imaging in Medicine and Surgery*. He received the E. K. Zavoisky Stipend from the ISMRM Scientific Meeting in 2014 and 2016, the Swedish Wenner-Gren Fellowship in 2014, and the Faculty Research Award at Xiamen University in 2014, respectively.